ISSN 1027-4510, Journal of Surface Investigation: X-ray, Synchrotron and Neutron Techniques, 2023, Vol. 17, No. 3, pp. 673–680. © Pleiades Publishing, Ltd., 2023.
Russian Text © The Author(s), 2023, published in Poverkhnost', 2023, No. 6, pp. 52–59.

Synthesis and Investigations of the Morphology and Structure of Fe_2O_3 Nanocoatings on Porous Al_2O_3 Obtained by the Oxidation of Magnetron-Deposited Fe Films

R. G. Valeev[a], *, A. N. Beltiukov[a], A. I. Chukavin[a], M. A. Eremina[a], and V. V. Kriventsov[b]

[a] *Udmurt Federal Research Center, Ural Branch, Russian Academy of Sciences, Izhevsk, 426008 Russia*

[b] *Federal Research Center, Boreskov Catalysis Institute, Siberian Branch, Russian Academy of Sciences, Novosibirsk, 630090 Russia*

**e-mail: rishatvaleev@mail.ru*

Received October 11, 2022; revised December 17, 2022; accepted December 17, 2022

Abstract—The results of studying the morphology and crystalline, local atomic, and chemical structure of iron(III) oxide coatings on the surface of porous aluminum oxide with different morphology using methods of scanning-electron- and atomic-force microscopy, X-ray phase analysis, X-ray photoelectron spectroscopy, as well as X-ray absorption near edge structure (XANES) spectroscopy are presented. Films of porous alumina are synthesized by the two-stage anodic oxidation of aluminum in 0.3 M aqueous solutions of sulfuric and oxalic acids. To change the pore diameter, some of the films are etched in a phosphoric-acid solution. Samples of iron oxide nanocoatings are obtained by oxidation of iron films in air deposited onto porous alumina substrate matrices by magnetron sputtering at a temperature of 300°C for 3 h. It is shown that oxidation leads to a twofold increase in the coating thickness of the control sample and is associated with an increase in the density of iron oxide compared to pure iron. With a change in the nanoporous structure on the surface of the substrates, the morphological features of the coatings change: there is overgrowth of the pores with iron oxide. Controlling the processes leading to such overgrowth will make it possible to carry out a targeted change in the structure-sensitive properties of composite structures based on iron oxide.

Keywords: iron oxide, porous alumina, coating, magnetron deposition, electron microscopy, atomic-force microscopy, X-ray photoelectron spectroscopy, X-ray absorption near edge structure spectroscopy

DOI: 10.1134/S1027451023030333

INTRODUCTION

Despite their long history, after the discovery of iron oxides as functional materials for various applications, interest in them has not decreased both in fundamental and applied science. Nanoparticles are actively studied for applications in medicine as active centers in magnetic resonance imaging [1], in targeted drug delivery [2], and for the processing of organic compounds [3], including oil [4], in catalysis. Films based on iron oxide have become widespread in magnetic recording devices [5], gas sensors [6], electrode materials [7], and optics [8].

Nevertheless, the search continues for new forms of materials with a characteristic size of structural features up to 500 nm, for example, obtained using surfaces with a highly porous structure (with a ratio of the area occupied by the pores to the area of the oxide film of more than 30%). One of these materials is porous anodic alumina, which has a structure with a highly ordered arrangement of pores vertically oriented toward the surface [9, 10] and is actively used as a template for the synthesis of various materials [11–14].

Earlier, we studied the structure and cathode properties of iron coatings deposited onto porous alumina by thermal deposition [15]. Magnetron films of materials, in contrast to thermally deposited ones, have more stable properties due to better control over the deposition process. It was noted [16] that during the thermal corrosion of a powder consisting of spherical iron particles with a diameter of 1–3 μm, materials with a metal–oxide shell structure are formed, but when oxidizing smaller particles with a diameter of up to 20 nm or coatings consisting of such particles with a thickness of no more than 200 nm, they can be completely oxidized. An analysis of the published data showed a complete lack of studies of the structure and

functional (cathode and magnetic) properties of nanostructured iron films, which determines their novelty.

Thus, the aim of this investigation is to study the morphology, structural and chemical state, and chemical composition of iron-oxide coatings on aluminum oxide with different morphology of the porous surface. In the future, the influence of these characteristics on the functional (magnetic, optical, membrane, and biocompatibility) properties of coatings will be revealed.

EXPERIMENTAL

Films of porous anodic alumina synthesized at a voltage of 25 V in a 0.3 M solution of sulfuric (H_2SO_4) acid and a voltage of 40 V in a 0.3 M solution of oxalic ($C_2H_2O_4$) acid were used as substrates for obtaining iron-oxide coatings with a nanostructured surface [9]. In total, three substrate samples were fabricated at an anodizing voltage of 40 V, two of which were etched for 30 and 50 min to increase the pore diameter, and one sample was fabricated at an anodizing voltage of 25 V. It should be noted that etching also slightly reduces the thickness of the porous film, which does not affect the final result of the study. An AKIP 1134-300-5 power supply was used as the voltage source. Synthesis was carried out in a refrigerator at an electrolyte temperature of 5°C, which made it possible to obtain an aluminum-oxide surface with hexagonally ordered pores with average diameters of 39 ± 2 and 50 ± 2 nm and distances between the pore centers of 64 ± 3 and 96 ± 3 nm for the initial films (before etching) of porous anodic alumina obtained by anodizing at voltages of 25 and 40 V. After etching, the average pore diameters increased to 60 ± 3 and 73 ± 3 nm, respectively. An iron film deposited onto a smooth polycor substrate was used as the sample for comparison. The coating thickness on the "smooth" substrate measured using atomic-force microscopy (AFM) by the height difference on a specially formed "step" was 28 ± 3 nm.

The deposition of iron was carried out by magnetron sputtering using an upgraded VUP-5 universal vacuum setup. The vacuum chamber of the setup was evacuated to an ultimate pressure of no worse than 10^{-6} mbar, the plasma discharge was ignited at a partial argon pressure of 5×10^{-3} mbar, and the cathode current was maintained at 100 mA at a voltage of about 220 V. A 99.9% iron target (TOO Girmet) was used as the evaporated material. The substrates were fixed at a distance of 100 mm from the magnetron. The substrates were annealed at a temperature of 250°C for 2 h before deposition for better adhesion of the coatings and the removal of adsorbed carbon contaminants; deposition was carried out on heated substrates. The samples were removed from the deposition chamber after nitrogen purging, which made it possible to exclude the process of abrupt oxidation of the surface of the iron coatings.

Oxidation in air was carried out using an SK2D-2-12TRA2 tube furnace (China) with two controlled heating zones at a temperature of 300°C for 3 h. The annealing temperature and time were chosen based on the assumption [17] that, in the temperature range from 250 to 300°C, the surface of pure iron is guaranteed to be oxidized. The heating rate was 10°C/min, and the cooling time to room temperature after annealing was about 5 h. After being removed from the oven, the coatings changed color from gray to yellow. Repeated measurement of the coating thickness after oxidation showed its increase to 60 ± 9 nm.

Studying the chemical state of iron in the coatings before and after annealing was carried out using X-ray photoelectron spectroscopy (XPS) on a Specs X-ray electron spectrometer. Electron emission was excited using AlK_α radiation (E = 1486.6 eV).

X-ray phase analysis of the coatings was carried out on a Rigaku MiniFlex 600 diffractometer using CoK_α radiation in the Bragg–Brentano geometry and θ–2θ configuration. The scanning step was 0.02°, and the scanning speed was 3 deg/min.

The surface morphology was studied by AFM and scanning-electron microscopy (SEM) using a software and hardware system based on an NT-MDT Integra Solaris atomic-force microscope in the tapping mode and a Thermo Fisher Scientific Quattro S scanning-electron microscope with a field-emission electron gun equipped with an energy-dispersive-analysis system based on an EDAX Octane Elect Plus EDS System spectrometer.

XANES (X-ray absorption near edge structure) studies were carried out in the fluorescence output mode using the EXAFS-spectroscopy experimental station, channel 8 of the VEPP-3 storage ring at the Center for Collective Use of the Siberian Center for Synchrotron Radiation, Novosibirsk. A Si(111) crystal was used to monochromatize the radiation. The XANES spectra for all studied samples were obtained at the K absorption edge of Fe (E_K = 7112 eV). The step in measuring the spectra was ~0.5 eV. The spectra were processed using the Viper (XANDA) software package [18].

RESULTS AND DISCUSSION

The film on the sample with a "smooth" substrate was studied by XPS (Fig. 1) to confirm the metallic state of the initial iron coatings and coatings after oxi-

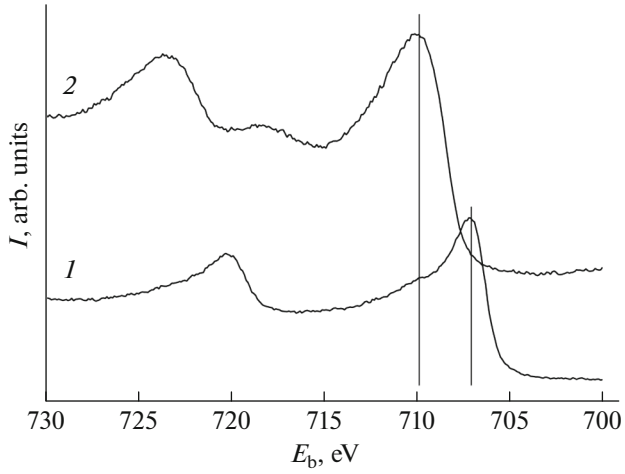

Fig. 1. XPS spectrum of the Fe film deposited on the polycor substrate (*1*) before and (*2*) after annealing. The vertical lines indicate the energy positions of the Fe^0 (E_b = 707 eV) and Fe^{3+} (E_b = 710 eV) lines.

dation. It can be seen that the initial film (curve *1*) is almost pure iron ($\Delta E(Fe2p_{1/2}–Fe2p_{3/2})$ = 13.2 eV), and after oxidation (curve *2*) corresponds to the spectrum of oxide Fe_2O_3 ($\Delta E(Fe2p_{1/2}–Fe2p_{3/2})$ = 13.6 eV) [19].

Figure 2 shows the diffraction patterns of the samples before and after annealing. The intensity of the reflection lines corresponding to the materials under study is rather weak due to the small thickness of the coatings; however, the lack of iron-oxide reflections on films before annealing, as well as the absence of iron reflections on the films after annealing, confirm the complete oxidation of iron on all substrates.

As can be seen from the SEM images (Fig. 3, center), iron deposition occurs predominantly in the area of porous aluminum-oxide films between the pores. As the AFM images show (Fig. 4), the coatings consist of clusters up to several tens of nm in size. In general, this is consistent with our earlier obtained data [15]. Images of the surface of the initial aluminum-oxide films are also shown in Fig. 3 (left).

After annealing at a temperature of 300°C for 3 h, pores are "overgrown" with iron oxide (Fig. 3, right). This is due to the fact that during the formation of oxide, the volume of the film increases, which is confirmed by a twofold increase in the thickness of the film on the polycor compared with the thickness of the initial iron film. Indeed, the density of iron is 7.87 g/cm^3, and that of Fe_2O_3 oxide is 5.24 g/cm^3, which can justify an increase in thickness by a maximum of 1.5 times. However, since the films are not continuous, but consist of clusters (Fig. 5), during

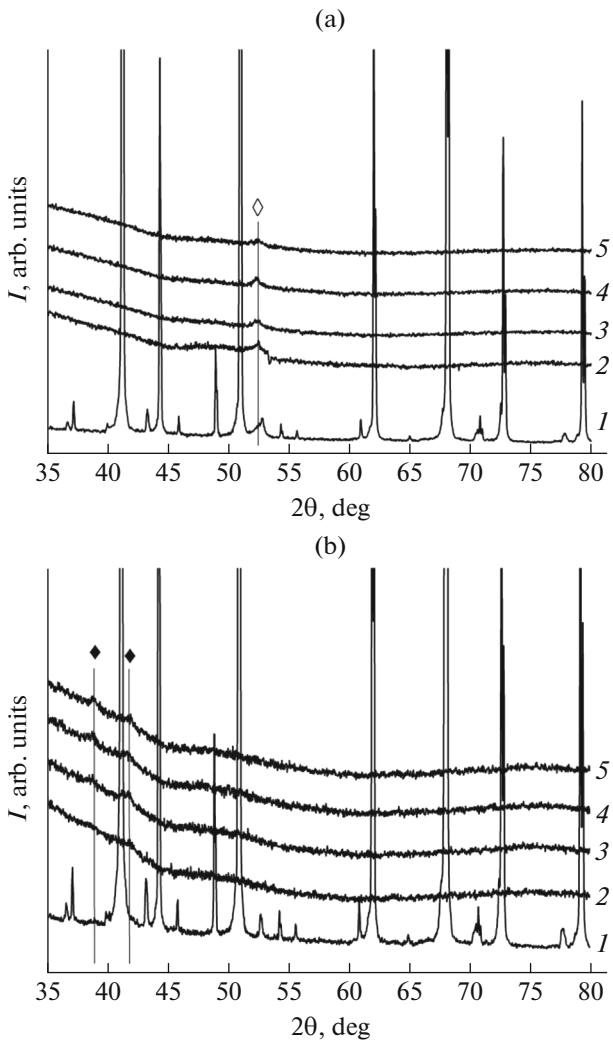

Fig. 2. X-ray diffraction patterns of (a) iron and (b) iron-oxide coatings on (*1*) polycor and (*2–5*) porous alumina substrates obtained (*2*) at 25 V, (*3*) 40 V, (*4*) 40 V followed by etching for 30 min, and (*5*) 40 V followed by etching for 50 min. The diffraction pattern shows the lines of (◇) Fe (110) and (◆) Fe_2O_3 (104) and (110).

annealing, along with an increase in the size of the particles themselves due to oxidation, there is an increase in voids between them, which justifies a twofold (from 28 ± 3 to 60 ± 9 nm) increase in the coating thickness. Planned further studies by XPS with layer-by-layer etching of the coatings will make it possible to determine the approximate depth, to which iron oxide penetrates into the pores of the matrix.

A coating sample obtained by the oxidation of iron on a porous anodic alumina matrix at 40 V followed by etching for 30 min was studied by XANES spectroscopy (Fig. 6) in order to finally confirm the fact of the formation of precisely Fe_2O_3 after annealing. The

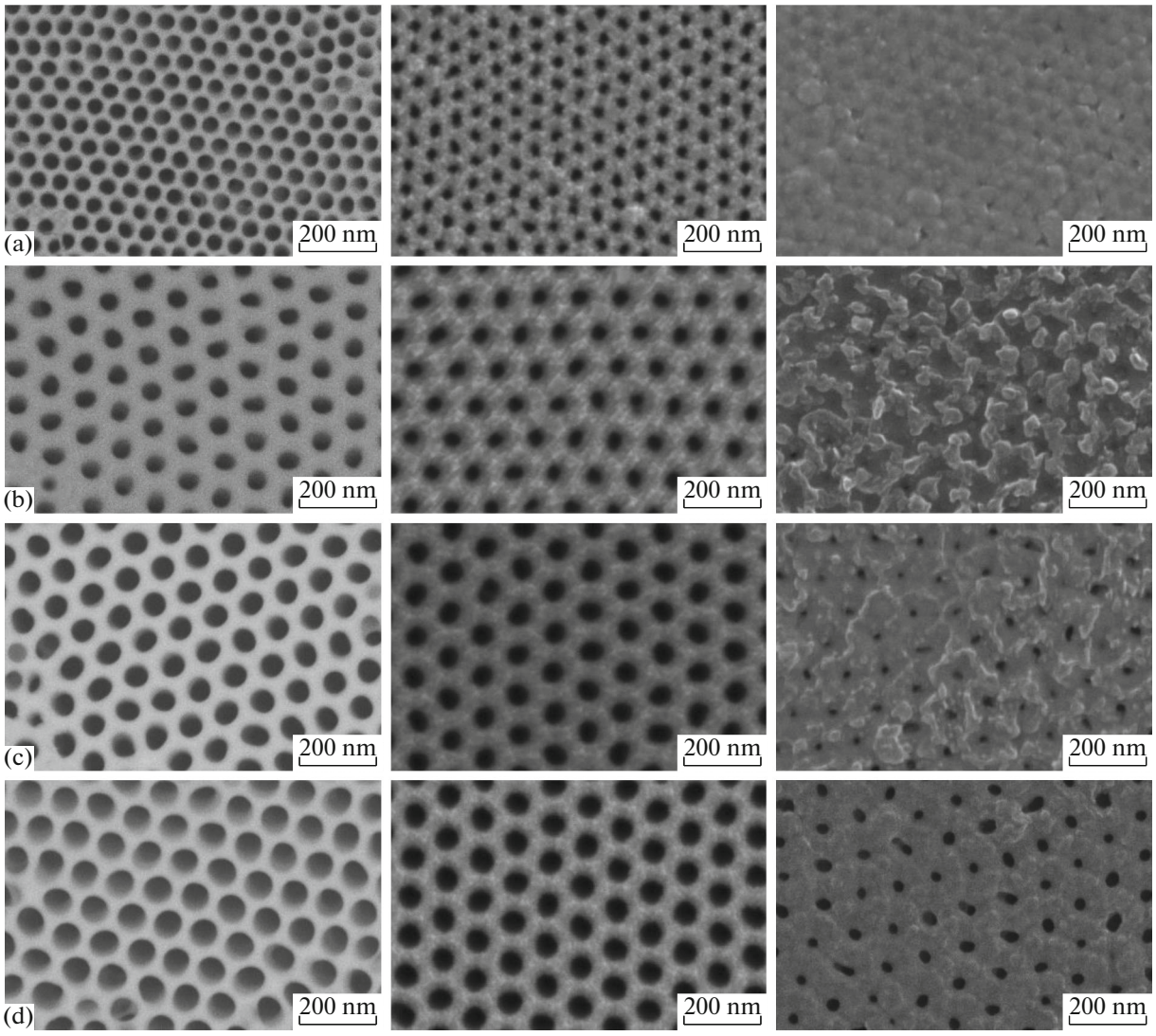

Fig. 3. SEM images of the initial films of porous alumina (left), Fe coatings deposited onto them (in the center) and Fe_2O_3 after oxidation in air (right): porous anodic alumina obtained (a) at 25 V, (b) 40 V, (c) 40 V followed by etching for 30 min, and (d) 40 V followed by etching for 50 min.

spectrum of the sample is presented in comparison with the spectra of the reference standards: iron oxide(III) and iron foil.

From a comparative analysis of the XANES spectra, it was found that the position of the absorption edge (~7116 eV) and the nature of the main features of the spectrum of the coating sample are in good agreement with those for the spectrum of the Fe_2O_3 reference standard. Since the samples are quite thin, it can be argued that the emission of photons in the fluorescence output shooting mode occurs from the entire thickness of the coating. It should be noted that the contributions to the spectrum of oxide phases FeO, Fe_3O_4, as well as metallic iron Fe^0 were not detected within the error of the method.

It should be noted that the mechanism of low-temperature (from 150 to 300°C) oxidation of thin iron films deposited onto substrates of another material has not yet been described in detail. It is known [20] that when iron is oxidized at temperatures of 250–300°C, magnetite Fe_3O_4 is formed directly on the metal surface and hematite Fe_2O_3 is formed on it. In the case of the oxidation of thin films and iron nanoparticles, the mechanism may differ; as is shown by the results presented in this study, Fe_2O_3 oxide is formed in the entire

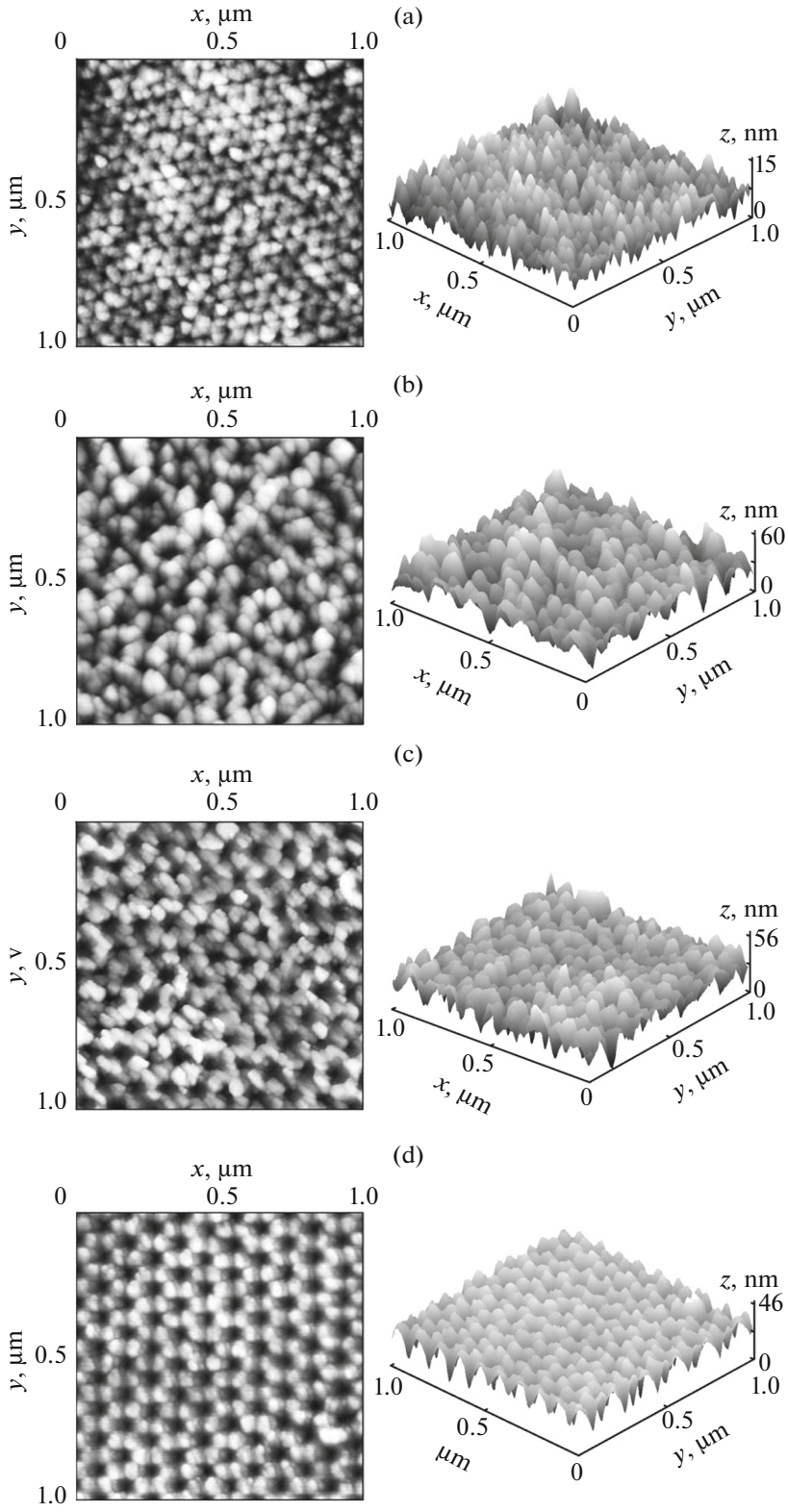

Fig. 4. 2D and 3D AFM images of Fe_2O_3 coatings on a porous anodic alumina substrate obtained at (a) 25 V, (b) 40 V, and (c) 40 V followed by etching for 30 min, and (d) 40 V followed by etching for 50 min.

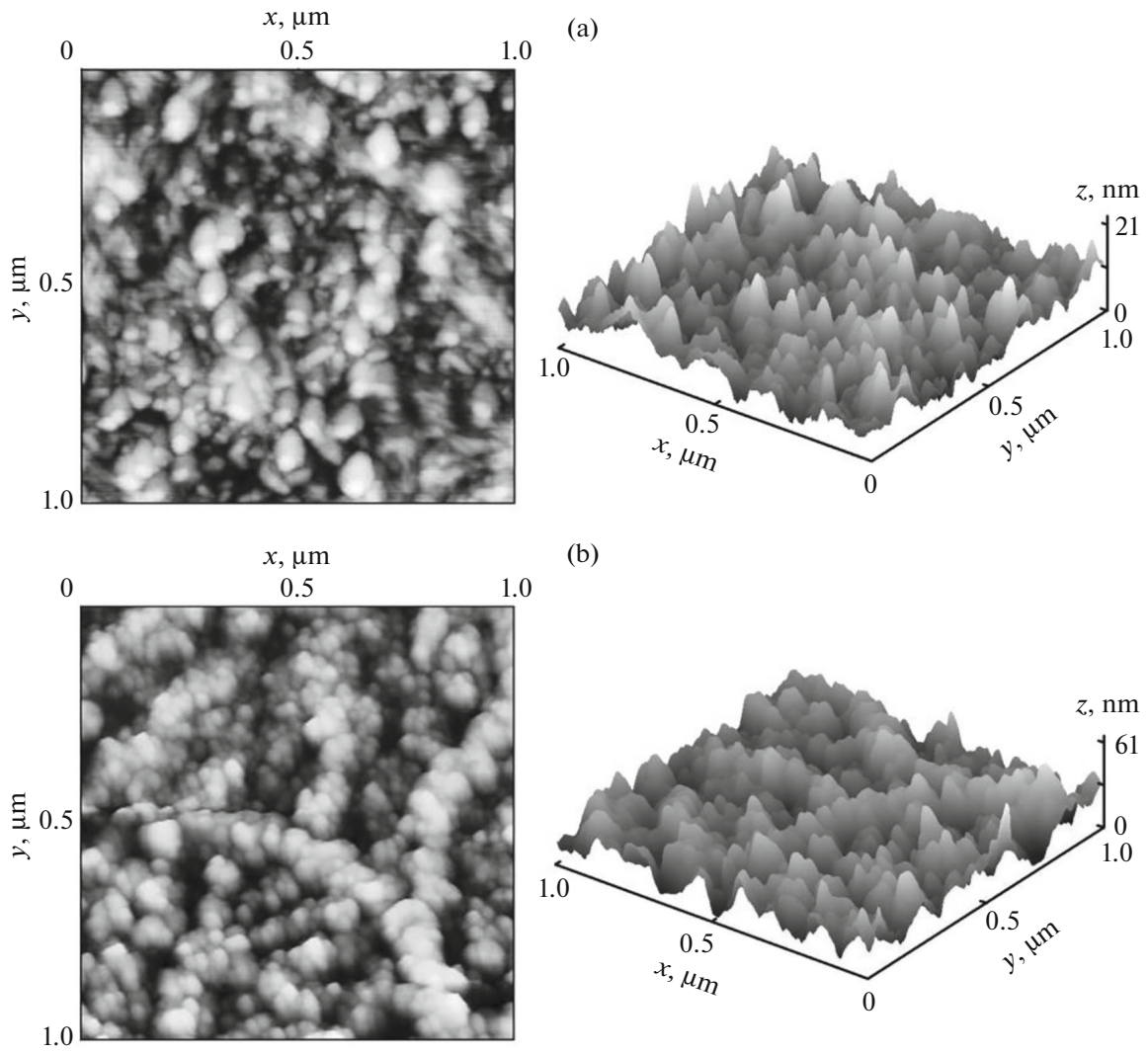

Fig. 5. 2D and 3D AFM images of (a) Fe and (b) Fe_2O_3 coatings on a polycor substrate.

metal layer, which requires separate experimental and theoretical studies.

CONCLUSIONS

A study of the morphology, structural and chemical state, and chemical composition of iron-oxide coatings on aluminum oxide with different porous surface morphology was carried out. It was shown that the deposition of iron occurs mainly in the area of porous films of aluminum oxide between the pores and the coatings consist of clusters up to several tens of nm in size. After annealing the iron coatings at a temperature of 300°C for three hours, overgrowth of the pores by iron oxide was found associated with an increase in the volume of films due to a change in their density, which is confirmed by a twofold increase in the thickness of the oxide film on the polycor surface compared to the thickness of the initial (before annealing) iron film, but establishing the exact mechanism of oxidation requires additional experimental and theoretical studies. X-ray diffraction analysis, XPS, and XANES confirmed that annealing results in the formation of a coating of Fe_2O_3 oxide; in this case, with a change in the morphology of the surface of the substrates, a change in the morphological features of the coatings occurs, in particular, a decrease in the pore diameter on the surface and an increase in the size of oxide particles compared to nonoxidized iron, which will make it possible to carry out a targeted change in the structure-sensitive properties of composite structures based on iron oxide.

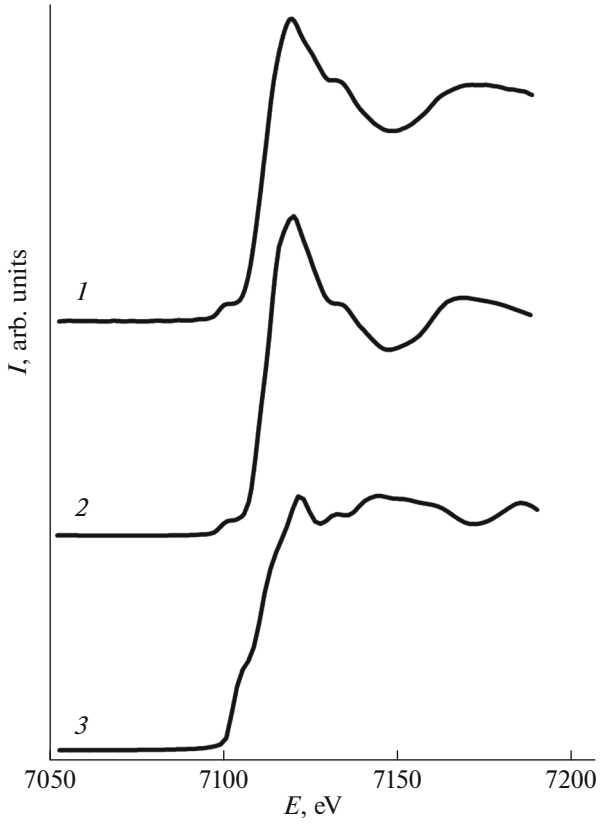

Fig. 6. XANES spectra of the studied Fe_2O_3 coating samples on porous anodic alumina obtained (*1*) at 40 V followed by etching for 30 min, (*2*) standard Fe_2O_3, and (*3*) Fe foils.

ACKNOWLEDGMENTS

The studies were carried out using the equipment of the Center for Collective Use "Center for Physical and Physical and Chemical Methods of Analysis, Study of the Properties and Characteristics of Surfaces, Nanostructures, Materials, and Products", Udmurt Federal Research Center, Ural Branch, Russian Academy of Sciences.

FUNDING

The study was supported by the Ministry of Science and Higher Education of Russia under agreement no. 075-15-2021-1351.

V.V. Kriventsov is thankful to the Ministry of Science and Higher Education of the Russian Federation for financial support within the framework of the state task for the Institute of Catalysis of the Siberian Branch of the Russian Academy of Sciences. Synchrotron studies were carried out using equipment of the Center for Collective Use "Siberian Center for Synchrotron Radiation" based on VEPP-4–VEPP-2000 at the Institute of Nuclear Physics, Siberian Branch, Russian Academy of Sciences with the financial support of the state task of the Institute of Catalysis, Siberian Branch, Russian Academy of Sciences.

CONFLICT OF INTEREST

The authors declare that they have no conflicts of interest.

REFERENCES

1. C. Chen, J. Ge, Y. Gao, C. Lei, J. Cui, J. Zeng, and M. Gao, Wiley Interdiscip. Rev.: Nanomed. Nanobiotechnol. **14**, 1740 (2022). https://www.doi.org/10.1002/wnan.1740
2. M. G. el Schneider, M. J. Martin, J. Otarola, E. Vakarelska, V. Simeonov, V. Lassalle, and M. Nedyalkova, Pharmaceutics **14**, 204 (2022). https://www.doi.org/10.3390/pharmaceutics14010204
3. P. Kumar, V. Tomar, D. Kumar, JoshiR. Kumar, and M. Nemival, Tetrahedron **106–107**, 132641 (2022). http://www.doi.org/10.1016/j.tet.2022.132641
4. F. Yakasai, M. Z. Jaafar, S. Bandyopadhyay, A. Agi, and M. A. Sidek, J. Pet. Sci. Eng. **208**, 109438 (2022). https://www.doi.org/10.1016/j.petrol.2021.109438
5. C. D. Powell, A. W. Lounsbury, Z. S. Fishman, C. L. Coonrod, M. J. Gallagher, D. Villagran, J. B. Zimmerman, L. D. Pfefferle, and M. S. Wong, Nano Convergence **8**, 8 (2021). http://www.doi.org/10.1186/s40580-021-00258-7
6. N. Song, H. Jiang, T. Cui, L. Chang, and X. Wang, Micro Nano Lett. **7**, 943 (2012). https://www.doi.org/ 10.1049/mnl.2012.0631
7. B. Sun, J. Horvat, H. S. Kim, W.-S. Kim, J. Ahn, and G. Wang, J. Phys. Chem. C **114**, 18753 (2010). https://www.doi.org/10.1021/jp102286e
8. A. Kumar and Y. Kamlesh, Mater. Res. Express **4**, 075003 (2017). https://www.doi.org/10.1088/2053-1591/aa75e9
9. K. S. Napolskii, I. V. Roslyakov, A. Y. Romanchuk, O. O. Kapitanova, A. S. Mankevich, V. A. Lebedev, and An. A. Eliseev, J. Mater. Chem. **22**, 11922 (2012). https://www.doi.org/10.1039/C2JM31710A
10. I. V. Roslyakov, A. P. Chumakov, An. A. Eliseev, A. P. Leontiev, O. V. Konovalov, K. S. Napolskii, J. Phys. Chem. C **125**, 9287 (2021). http://www.doi.org/10.1021/acs.jpcc.1c01482
11. A. Ruiz-Clavijo, O. Caballero-Calero, and M. Martín-González, Nanoscale **13**, 2227 (2021). https://www.doi.org/10.1039/D0NR07582E
12. R. G. Valeev, A. L. Trigub, Ya. V. Zubavichus, F. Z. Gil'mutdinov, I. A. El'kin, J. Surf. Invest.: X-ray, Synchrotron Neutron Tech. **11**, 879 (2017). https://doi.org/10.1134/S1027451017040310 https://www.doi.org/10.7868/S0207352817080145
13. A. I. Chukavin, R. G. Valeev, Ya. V. Zubavichus, A. L. Trigub, and A. N. Beltyukov, J. Struct. Chem. **58**, 1236 (2017). https://doi.org/10.1134/S0022476617060233

14. A. H. A. Elmekawy, E. G. Iashina, I. S. Dubitskiy, S. V. Sotnichuk, I. V. Bozhev, D. A. Kozlov, K. S. Napolskii, D. Menzel, and A. A. Mistonov, J. Magn. Magn. Mater. **532**, 167951 (2022). http://www.doi.org/10.1016/j.jmmm.2021.167951

15. R. G. Valeev and A. S. Alalykin, Nanotechnol. Russ. **14**, 346 (2019). https://doi.org/10.1134/S199507801904013X

16. V. A. Kotenev, M. R. Kiselev, V. V. Vysotskii, A. A. Averin, and A. Yu. Tsivadze, Prot. Met. Phys. Chem. Surf. **52**, 825 (2016). https://doi.org/10.1134/S2070205116050154

17. A. A. Ots, *Corrosion and Wear of Heating Surfaces of Boilers* (Energoatomizdat, Moscow, 1987) [in Russian].

18. K. V. Klementev, Nucl. Instrum. Methods Phys. Res., Sect. A **448**, 299 (2000). http://www.doi.org/10.1016/S0168-9002(99)00710-X

19. C. D. Wagner, W. M. Rigs, L. E. Davis, and J. F. Moulder, *Handbook of X-Ray Photoelectron Spectroscopy: A Reference Book of Standard Data for Use in X-Ray Photoelectron Spectroscopy*, Ed. by G. E. Muilenberg (Perkin-Elmer, Eden Prairie, 1979).

20. O. Kubaschewski and B. E. Hopkins, *Oxidation of Metals and Alloys* (Butterworths, London, 1953; Metallurgiya, Moscow, 1965).

Translated by S. Rostovtseva